Dynamics of Chemical Reactivity Indices for a Many-Electron System in Its Ground and Excited States

P. K. Chattaraj* and S. Sengupta

Department of Chemistry, Indian Institute of Technology, Kharagpur 721 302, India

Received: April 25, 1997; In Final Form: July 17, 1997[⊗]

A quantum fluid density functional approach is adopted to study the time evolution of various reactivity parameters such as electronegativity, hardness, polarizability, and entropy associated with a collision process between a proton and a Be atom in its ground and excited electronic states. This collision process may be considered to be a model mimicking the actual chemical reaction between a Be atom and a proton to give rise to a BeH^+ molecule. A favorable dynamical process involving a ground or an excited state is characterized by maximum hardness, minimum polarizability, and maximum entropy values.

I. Introduction

Electronegativity[1] (χ) and hardness[2] (η) are two important indices of chemical reactivity. Since inception these two quantities have been extensively used in understanding molecular structure, properties, reactivity, bonding, interactions, and dynamics. The concept of electronegativity was first introduced by Pauling[3] as the power of an atom in a molecule to attract electrons to itself, while that of hardness was given by Pearson[4] in the context of the hard−soft acid−base (HSAB) principle which states that "hard acids will prefer to react with hard bases and soft acids with soft bases to form a kinetically and thermodynamically stable molecule". Quantitative definitions of these properties are provided within the purview of density functional theory[5] (DFT). Electronegativity[6] and hardness[7] are respectively defined as the following first- and second-order derivatives,

$$\chi = -\mu = -\left(\frac{\partial E}{\partial N}\right)_{v(\mathbf{r})} \tag{1}$$

and

$$\eta = \frac{1}{2}\left(\frac{\partial^2 E}{\partial N^2}\right)_{v(\mathbf{r})} = \frac{1}{2}\left(\frac{\partial \mu}{\partial N}\right)_{v(\mathbf{r})} \tag{2}$$

for an N-electron system with energy E and chemical and external potentials μ and $v(\mathbf{r})$, respectively. Equivalently, hardness can be expressed as[8]

$$\eta = \frac{1}{N}\int\int \eta(\mathbf{r},\mathbf{r}')\, f(\mathbf{r}')\, \rho(\mathbf{r})\, d\mathbf{r}\, d\mathbf{r}' \tag{3}$$

where $f(\mathbf{r})$ is the Fukui function[9] and the hardness kernel is given by[8]

$$\eta(\mathbf{r},\mathbf{r}') = \frac{1}{2}\frac{\delta^2 F[\rho]}{\delta\rho(\mathbf{r})\,\delta\rho(\mathbf{r}')} \tag{4}$$

in terms of the Hohenberg−Kohn−Sham universal functional[10] $F[\rho]$ of DFT. There are some useful principles of molecular electronic structure based on these concepts. Electronegativity difference is the major driving force behind the electron-transfer processes in chemical reactions. Electrons are transferred from a species of lower electronegativity to one with higher electronegativity until the electronegativity values of both the species become equal. In a molecule, all the constituent atoms have the same electronegativity value which is equal to the geometric mean of the isolated atoms' electronegativities.[11] An important hardness-related principle is the maximum hardness principle[12] which states that "there seems to be a rule of nature that molecules arrange themselves so as to be as hard as possible". Theoretical justifications of all three principles, viz. electronegativity equalization,[13] HSAB,[7,14] and maximum hardness[15] principles have been provided within DFT.

The wave function of a many-particle system is completely characterized by N and $v(\mathbf{r})$. While χ and η measure the response of the system when N changes at fixed $v(\mathbf{r})$, polarizability (α) plays the same role for varying $v(\mathbf{r})$ at constant N. Owing to an inverse relationship[16] between α and η, a minimum polarizability principle in agreement with the maximum hardness principle has been first conjectured and then explicitly demonstrated in a time-dependent situation.[17] It may be stated as[17] "the natural direction of evolution of any system is towards a state of minimum polarizability". Validity of this principle in case of chemical reactions has also been shown.[18] Another important principle is that of maximum entropy[19] which states that "the most probable distribution is associated with the maximum value of the Shannon entropy of the information theory".

Dynamic generalizations of these principles have been studied and the possibility of a chemical reaction dynamics in terms of the time evolution of these quantities has been explored in our laboratory.[17,20] To our knowledge, no attempt has been made so far in extending these studies to excited states especially in the time-dependent situation. In the present paper we employ quantum fluid density functional theory[21] to study a collision process between an ion and an atom in its ground and excited electronic states and to monitor the time evolution of various reactivity parameters in order to gain insights into the associated structure principles in a dynamical context, involving both ground and excited states. Theoretical background of the present work is presented in section II. A new kinetic energy functional and a new Fukui function used for this purpose are described in sections III and IV, respectively. Section V provides numerical details, and the results and discussions are given in section VI. Finally, section VII contains some concluding remarks.

II. Theoretical Background

Hohenberg−Kohn−Sham density functional theory[10] was originally formulated for the ground state. It asserts that the electron density ($\rho(\mathbf{r})$) contains all the information of a system.

* Author for correspondence.

⊗ Abstract published in *Advance ACS Abstracts,* September 1, 1997.

S1089-5639(97)01408-4 CCC: $14.00

To tackle the dynamical situations, a time-dependent version of DFT is provided[22] which shows that the mapping between the time-dependent external potential and $\rho(\mathbf{r},t)$ is uniquely invertible, implying that all the properties of the system are functionals of $\rho(\mathbf{r},t)$ and current density $\mathbf{j}(\mathbf{r},t)$. Now a dynamical process can be studied in case we have an equation to obtain $\rho(\mathbf{r},t)$ and $\mathbf{j}(\mathbf{r},t)$ at all times. An amalgamation of time-dependent DFT[22] and quantum fluid dynamics[23] resulted in quantum fluid density functional theory[21] whose backbone is the following generalized nonlinear Schrödinger equation

$$\left[-\frac{1}{2}\nabla^2 + v_{\text{eff}}(\mathbf{r},t)\right]\Phi(\mathbf{r},t) = \mathrm{i}\,\frac{\partial\Phi(\mathbf{r},t)}{\partial t}, \quad \mathrm{i} = \sqrt{-1} \tag{5a}$$

with

$$\Phi(\mathbf{r},t) = \rho^{1/2}\exp(\mathrm{i}\xi); \qquad \mathbf{j} = [\Phi_{\text{re}}\nabla\Phi_{\text{im}} - \Phi_{\text{im}}\nabla\Phi_{\text{re}}] = \rho\nabla\xi \tag{5b}$$

where ξ is the velocity potential. In the present paper we solve this equation to study the temporal evolution of various reactivity parameters associated with a collision process between a proton and a Be atom in its ground and excited electronic states. We have chosen this system because in the presence of a third partner to take away the excess energy, this collision may lead to the formation of a stable closed shell molecule[24] BeH^+ with $D_0 = 3.14$ Ev and $R_e = 1.3122$ Å. In eq 5a the effective potential v_{eff} is given by

$$v_{\text{eff}}(\mathbf{r},t) = \left(\frac{\delta T_{\text{NW}}}{\delta\rho}\right) + \left(\frac{\delta E_{\text{xc}}}{\delta\rho}\right) + \int\frac{\rho(\mathbf{r}',t)}{|\mathbf{r}-\mathbf{r}'|}\,\mathrm{d}\mathbf{r}' - \frac{Z_1}{|\mathbf{R}_1(t)-\mathbf{r}|} - \frac{Z_2}{|\mathbf{R}_2(t)-\mathbf{r}|} \tag{6}$$

where T_{NW} and E_{xc} denote the non-Weizsäcker part of the kinetic energy and exchange−correlation energy functionals, respectively. The explicit form for T_{NW} is given in the next section and that of E_{xc} has been taken as

$$E_{\text{xc}}[\rho] = E_{\text{x}}[\rho] + E_{\text{c}}[\rho] \tag{7a}$$

where E_{x} is the Dirac exchange functional modified in the spirit of Becke's functional,[25] as follows[26]

$$E_{\text{x}}[\rho] = -C_{\text{x}}\left[\int\rho^{4/3}\,\mathrm{d}\mathbf{r} + \int\frac{\rho^{4/3}}{1+(\mathbf{r}^2\rho^{2/3}/0.0244)}\,\mathrm{d}\mathbf{r}\right], \qquad C_{\text{x}} = \left(\frac{3}{4\pi}\right)(3\pi^2)^{1/3} \tag{7b}$$

and E_{c} is a Wigner-type parametrized correlation energy functional given by[27]

$$E_{\text{c}}[\rho] = -\int\frac{\rho}{9.81 + 21.437\rho^{-1/3}}\,\mathrm{d}\mathbf{r} \tag{7c}$$

In eq 6 $\mathbf{R}_1$,$\mathbf{R}_2$ and Z_1,Z_2 are radius vectors and atomic numbers of the target (Be) and the projectile (H^+) nuclei, respectively. The origin of the coordinate system is fixed on the target nucleus, and the position of the projectile is determined by a Coulomb trajectory.[28]

Unique invertibility of the mappings $v_{\text{ext}}(\mathbf{r},t) \rightarrow \rho(\mathbf{r},t)$ and $v_{\text{ext}}(\mathbf{r},t) \rightarrow \mathbf{j}(\mathbf{r},t)$, $v_{\text{ext}}(\mathbf{r},t)$ being the external potential, has been established[22] in time-dependent DFT. Therefore, any time-dependent quantity is a unique functional of $\rho(\mathbf{r},t)$ and $\mathbf{j}(\mathbf{r},t)$. For the present problem the time-dependent energy may be written as

$$E(t) = \frac{1}{2}\int\rho(\mathbf{r},t)|\nabla\xi(\mathbf{r},t)|^2\,\mathrm{d}\mathbf{r} + T[\rho] + \frac{1}{2}\int\int\frac{\rho(\mathbf{r},t)\,\rho(\mathbf{r}',t)}{|\mathbf{r}-\mathbf{r}'|}\,\mathrm{d}\mathbf{r} + E_{\text{xc}}[\rho] - Z_1\int\frac{\rho(\mathbf{r},t)}{|\mathbf{R}_1-\mathbf{r}|}\,\mathrm{d}\mathbf{r} - Z_2\int\frac{\rho(\mathbf{r},t)}{|\mathbf{R}_2-\mathbf{r}|}\,\mathrm{d}\mathbf{r} \tag{8}$$

where the first term is the macroscopic kinetic energy and the second term is the intrinsic kinetic energy whose explicit form is given in the next section. Energy or any other time-dependent quantity at any given time step can be calculated in case $\rho(\mathbf{r},t)$ and $\mathbf{j}(\mathbf{r},t)$ are known at that time step. Quantum fluid density functional theory helps obtaining them through the solution of eq 5a,b.

Time evolution of electronegativity can be followed by writing it as follows,[17,20]

$$\chi(t) = -\mu(t) = -\frac{\delta E(t)}{\delta\rho} = -\left[\frac{1}{2}\left|\nabla\xi\right|^2 + \frac{\partial T}{\delta\rho} + \int\frac{\rho(\mathbf{r}',t)}{|\mathbf{r}-\mathbf{r}'|}\,\mathrm{d}\mathbf{r}' + \frac{\delta E_{\text{xc}}[\rho]}{\delta\rho}\right] + \frac{Z_1}{|\mathbf{R}_1-\mathbf{r}|} + \frac{Z_2}{|\mathbf{R}_2-\mathbf{r}|} \tag{9}$$

The time-dependent chemical potential becomes equal to the total electrostatic potential[17,20] at a point $\mathbf{r}_\mu$, i.e.,

$$-\chi(t) = \mu(t) = \int\frac{\rho(\mathbf{r},t)}{|\mathbf{r}_\mu-\mathbf{r}|}\,\mathrm{d}\mathbf{r} - \frac{Z_1}{|\mathbf{R}_1-\mathbf{r}_\mu|} - \frac{Z_2}{|\mathbf{R}_2-\mathbf{r}_\mu|} \tag{10}$$

where $\mathbf{r}_\mu$ is the point in which the following condition is satisfied at that time step,

$$\frac{1}{2}(\nabla\xi)^2 + \frac{\delta T}{\delta\rho} + \frac{\delta E_{\text{xc}}[\rho]}{\delta\rho} = 0 \tag{11}$$

It may be noted that at $t = 0$ eqs 9 and 10 transform to those given by Politzer et al.[29] to calculate the covalent radii of atoms using the electronegativity equalization principle. Note the misprints in eqs 6 and 8 of ref 17, in the potential term arising out of the macroscopic kinetic energy which, however, was calculated correctly.

Equations 3 and 4 have been used to study the hardness dynamics. The required Hohenberg−Kohn−Sham universal functional $F[\rho]$ to calculate the hardness kernel (eq 4) is taken from eq 8 by removing the external potential dependent terms. Section IV describes the Fukui function $f(\mathbf{r})$ employed in the present work to calculate the global hardness from eq 3. Note that a clear-cut maximum was not obtained in the time-dependent hardness profile in our earlier calculations[17,20] in which the homogeneous electron gas formula for $f(\mathbf{r})$ was used.[17,20]

To monitor the time evolution of polarizability we calculate it as follows

$$\alpha(t) = |\mathbf{D}^z_{\text{ind}}(t)|/|\mathbf{G}_z(t)| \tag{12}$$

where $\mathbf{D}^z_{\text{ind}}(t)$ is the electronic part of the induced dipole moment and $\mathbf{G}_z(t)$ is component of the external Coulomb field along the z axis. It has been legitimately assumed[17,20,21,28] that the overall charge distribution is cylindrically symmetric about an axis ($-\infty \le z \le \infty$) passing through the target nucleus, due to the high projectile velocity.

TABLE 1: Calculated Kinetic Energy Values (au) for Atomic Systems

atom	T_0[a]	T_0+T_2[a]	$T_0+T_2+T_4$[a]	T_0+T_r[b]	T_{GB}[c]	T_{GD}[d]	T_{PW}[e]	T_{HF}[f]
He	2.561	2.879	2.963	2.860	2.862	2.852	2.862	2.862
Li	6.673	7.467	7.662	7.426	7.566	7.416	7.568	7.433
Be	13.124	14.635	14.990	14.563	14.975	14.537	14.986	14.573
C(^{1}D)	33.608	37.156	37.942	37.077	37.899	37.057	37.924	37.688
N	48.312	53.115	54.490	53.111	54.284	53.384	53.721	54.401
Ne	117.76	127.83	129.78	128.13	128.47	128.04	128.491	128.55
Mg	183.99	198.71	201.49	199.36	199.55	199.28	199.663	199.61
Ar	489.95	524.22	530.43	526.58	527.47	526.57	527.252	526.81
Kr	2591.18	2733.04	2757.10	2749.44	2749.3	2750.9	2748.823	2752.0
Xe	6857.74	7183.52	7237.25	7228.19	7235.3	7233.4	7235.147	7232.0

[a] References 34 and 36. [b] Reference 34. [c] Reference 37. [d] Reference 26. [e] Present work. [f] Hartree−Fock kinetic energy values from ref 35.

To study the entropy dynamics, an average density argument[17,20,21] is used for its definition. Considering an N-electron system as a system of N noninteracting particles moving under the influence of an effective potential field $v_{\text{eff}}(\mathbf{r},t)$, entropy is defined as[17,20,21]

$$S(t) = \int \{^5/_2 - \ln \rho(\mathbf{r},t) + {}^3/_2 \ln(k\theta(\mathbf{r},t)/2\pi)\} k\rho(\mathbf{r},t)\, d\mathbf{r} \quad (13)$$

In eq 13 k is the Boltzmann constant and $\theta(\mathbf{r},t)$ is a space−time-dependent temperature given as[17,20,21]

$$t_s(\mathbf{r};\rho(\mathbf{r},t)) = {}^3/_2 k\, \theta(\mathbf{r},t)\, \rho(\mathbf{r},t) + \left(\frac{|\mathbf{j}(\mathbf{r},t)|^2}{2\rho(\mathbf{r},t)}\right) \quad (14)$$

where $t_s(\mathbf{r};\rho(\mathbf{r},t))$ is the kinetic energy density which integrates to the total kinetic energy as prescribed in the next section.

III. A New Kinetic Energy Functional

Although the Hohenberg−Kohn theorem asserts the existence of an energy functional, the exact forms for kinetic and exchange−correlation energy functionals are still not known.[30] Attempts have been made to construct approximate kinetic energy functionals with good local and global behavior as well as a proper functional derivative.[30] Recently, Ghosh and Deb[26] have proposed a new local kinetic energy functional as follows

$$T[\rho] = T_0[\rho] + C_x \int \frac{\rho^{4/3}/\mathbf{r}}{1 + (\mathbf{r}\rho^{1/3}/0.043)}\, d\mathbf{r} \quad (15)$$

where $T_0[\rho]$ is the Thomas−Fermi functional given by

$$T_0[\rho] = C_k \int \rho(\mathbf{r})^{5/3}\, d\mathbf{r}; \quad C_k = {}^3/_{10}(3\pi^2)^{2/3} \quad (16)$$

Considering the importance[31,32] of the Weizsäcker functional $T_W[\rho]$ and a global correlation[33] between a first gradient correction[34] and the above local correction,[26] we propose the following functional with proper global and local behavior and the correct functional derivative,[26]

$$T_{PW}[\rho] = T_0[\rho] + T_W[\rho] - a(N)\lambda \int \frac{\rho^{4/3}/\mathbf{r}}{1 + (\mathbf{r}\rho^{1/3}/0.043)}\, d\mathbf{r} \quad (17a)$$

where

$$T_W[\rho] = \frac{1}{8}\int \frac{\nabla\rho\cdot\nabla\rho}{\rho}\, d\mathbf{r} \quad (17b)$$

$$\lambda = 30\left(\frac{3}{\pi}\right)^{1/3} \quad (17c)$$

$$a(N) = a_0 + a_1 N^{-1/3} + a_2 N^{-2/3};$$
$$a_0 = 0.1279,\ a_1 = 0.1811,\ a_2 = -0.0819 \quad (17d)$$

Total kinetic energy values for several atoms have been calculated using near-Hartree−Fock atomic densities[35] in eq 17. Table 1 compares these values with other values obtained from existing important kinetic energy functionals. If we consider the importance[31,32] of $T_W[\rho]$ and both global and local behavior as well as the behavior of the functional derivative[26,30] of the present functional, it (eq 17) serves as one of the best kinetic energy functionals known to date. Note that the local behavior may be further improved by adding a fraction of $\nabla^2\rho$ term such that the global values are not disturbed.

To tackle a molecular situation we add[17,20,21] another term to $T_{PW}[\rho]$ as

$$T[\rho] = T_{PW}[\rho] + \int t_{mol}[\rho]\, d\mathbf{r} \quad (18a)$$

where

$$t_{mol}[\rho] = \int (\psi(R,N)/N^2)\, \rho(\mathbf{r})\, \rho(\mathbf{r}')\, d\mathbf{r}' \quad (18b)$$

$$\psi(R,N) = \frac{1}{R^{12}} - \left(\frac{N}{10}\right)^{14} R^2 \exp(-0.8R) \quad (18c)$$

The molecular kinetic energy functional is designed in such a way that $t_{mol}[\rho]$ goes to 0 when R tends to infinity and diatomic molecular kinetic energy values are reproduced at the equilibrium bond lengths.[17,20,21]

IV. A Local Model for the Fukui Function

The Fukui function[9] $f(\mathbf{r})$ is one of the most important chemical reactivity indices that brings the necessary simple quantification in Fukui's frontier orbital theory[38] by characterizing the most reactive site of a chemical species with that having the largest value of $f(\mathbf{r})$. It is defined as follows[9]

$$f(\mathbf{r}) = \left(\frac{\partial\rho(r)}{\partial N}\right)_{v(\mathbf{r})} = \left(\frac{\delta\mu}{\delta v(\mathbf{r})}\right)_N \quad (19)$$

Because of the difficulties associated with the calculations of the above derivatives there have been several attempts[17,20,39,40] to express $f(\mathbf{r})$ as a density functional such that it can be calculated straightforward with only the electron density of the species concerned as input. A completely satisfactory Fukui density functional for practical atomic and molecular calculations is, however, still awaited. Recently, Fuentealba[40] has proposed a local model for $f(\mathbf{r})$. In the present work we propose a form for $f(\mathbf{r})$ in a somewhat similar manner using better quality energy functionals. Ultimately this $f(\mathbf{r})$ will be used in the calculation of global hardness. To model $f(\mathbf{r})$ we take the

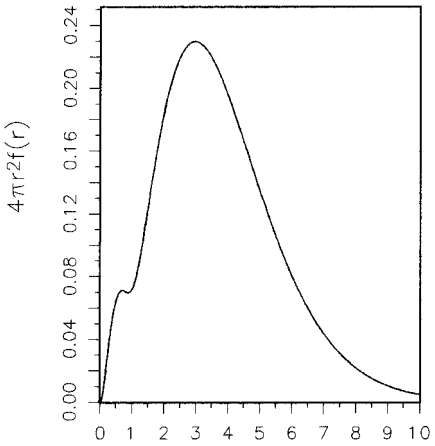

Figure 1. Radial distribution of the Fukui function for the Be atom.

following Hohenberg−Kohn−Sham universal functional, viz.,

$$F[\rho] = T[\rho] + V_{ee}[\rho] \tag{20}$$

where $T[\rho]$ and the total electron−electron repulsion energy $V_{ee}[\rho]$ are taken, respectively, as in eq 15 and the following local formula given by Parr,[41]

$$V_{ee}[\rho] = 0.7937(N-1)^{2/3}\int \rho(\mathbf{r})^{4/3}\, d\mathbf{r} \tag{21}$$

Equations 4 and 20 give the hardness kernel $\eta(\mathbf{r},\mathbf{r}')$ which is related to the local softness $s(\mathbf{r})$ within this local model as follows,[40]

$$s(\mathbf{r}) = \frac{\delta(\mathbf{r}-\mathbf{r}')}{2\eta(\mathbf{r},\mathbf{r}')} \tag{22}$$

The Fukui function can now be easily obtained as the normalized $s(\mathbf{r})$, i.e.,

$$f(\mathbf{r}) = \frac{s(\mathbf{r})}{\int s(\mathbf{r})\, d\mathbf{r}} \tag{23}$$

A local hardness can also be obtained by averaging over $\eta(\mathbf{r},\mathbf{r}')$ as[8,40]

$$\eta(\mathbf{r}) = \frac{1}{N}\int \eta(\mathbf{r},\mathbf{r}')\,\rho(\mathbf{r}')\, d\mathbf{r}' = \frac{1}{2N}\frac{\rho(\mathbf{r})}{s(\mathbf{r})} \tag{24}$$

Figure 1 depicts the radial distribution of $f(\mathbf{r})$ for a Be atom calculated using eq 23 by employing a near-Hartree−Fock atomic density.[35] The presence of atomic shell structure is discernible. It is important to note that the Fukui function is positive everywhere.

Radial distributions of local hardness for several noble gas atoms are presented in Figure 2. Near-Hartree−Fock atomic densities[35] and eq 24 are used for this purpose. Atomic shell structure is very prominent in these plots. It complements our previous observation[20] that $\eta(\mathbf{r})$ plots resemble density plots more than $(-\nabla^2\rho)$ plots[42] to predict the hard−soft behavior of an atom or a molecule. This behavior is in conformity with the fact that the hard−hard interactions are charge-controlled.[43] It has also been shown[44] through ab initio molecular orbital calculations that the harder nitrogen end in the linkage isomer SCN^- possesses maximum gross charge.

V. Numerical Solution

Due to the high projectile velocity we legitimately assume the azimuthal symmetry of the whole scattering system. Since

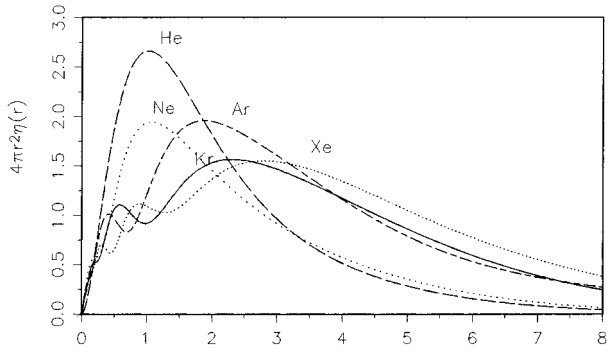

Figure 2. Radial distribution of the local hardness for the noble gas atoms.

the electron density varies rapidly near the nucleus and relatively slowly elsewhere we transform the variables as follows

$$y = \tilde{\rho}\Phi \tag{25a}$$

and

$$\tilde{\rho} = x^2 \tag{25b}$$

where $\tilde{\rho}$ is one of the cylindrical polar coordinates $(\tilde{\rho},\tilde{\varphi},z)$. An analytical integration has been carried out over $0 \le \tilde{\varphi} \le 2\pi$. The generalized nonlinear Schrödinger eq 5a takes the following form[20,21] in transformed variables

$$\left\{\left(\frac{3}{4x^3}\right)\frac{\partial y}{\partial x} - \left(\frac{1}{4x^2}\right)\frac{\partial^2 y}{\partial x^2} - \frac{\partial^2 y}{\partial z^2}\right\} - \left(\frac{1}{x^4} - 2\nu_{\text{eff}}\right)y = 2\mathrm{i}\,\frac{\partial y}{\partial t} \tag{26}$$

A leapfrog-type finite difference scheme has been employed to numerically solve eq 26. A detailed discussion on the derivation of eq 26 and the numerical method for its solution can be found elsewhere.[20,21] The spatial and temporal grid sizes are taken as

$$\Delta x = \Delta z = 0.05 \text{ au} \quad \text{and} \quad \Delta t = 0.025 \text{ au}$$

The position of the Be nucleus is chosen to be the origin of the coordinate system. A proton with initial velocity 1 au is approaching the Be nucleus from a distance of 10 au along a Coulomb trajectory[28] with an impact parameter 0.1 au and the scattering angle 5.25°. The integration is carried out until the proton recedes by a distance of 10 au from the target. To launch the numerical solution we have taken the Be atom in ^1S and ^3P electronic states.[45] To our knowledge, the calculation of various local and global reactivity parameters in a time-dependent situation for a system in its excited state is done here for the first time.

VI. Results and Discussions

Temporal evolution of the electronic chemical potential (negative of electronegativity) is presented in Figure 3. Unless otherwise specified, in all figures parts a and b refer to ground and excited states of Be the atom, respectively. Time dependence of different quantities such as induced dipole moment and difference density helped[21] dividing the whole collision process into three distinct regions, viz., approach, encounter, and departure. Time evolution of μ also clearly marks these divisions. In the encounter regime where the actual chemical process takes place, eq 11 is not satisfied anywhere in the whole space. But for the initial transients and strong nonlinear fluctuations immediately before and after the encounter regime μ attains a more or less steady value in the approach and departure zones.

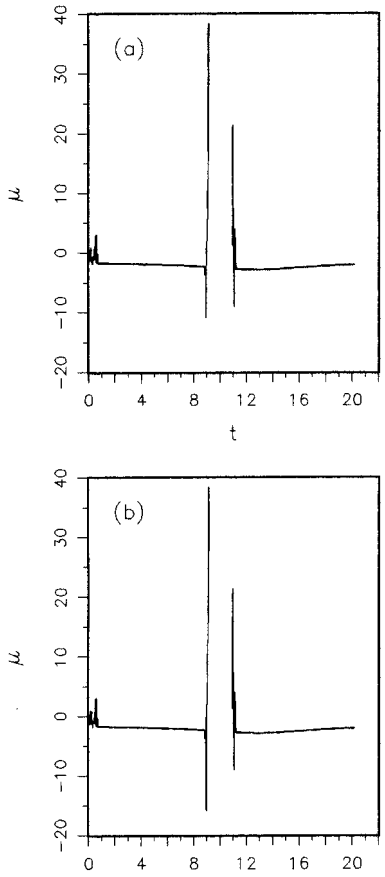

Figure 3. Time evolution of chemical potential (μ) during a collision process between a Be atom and a proton: (a) ground state, (b) excited state.

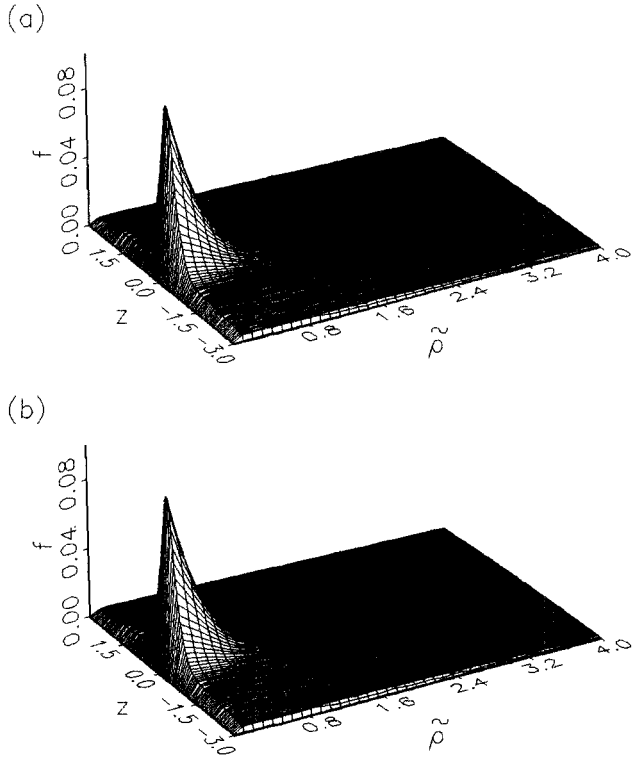

Figure 4. Perspective plots of the Fukui function of the Be atom colliding with a proton, at $t = 0$: (a) ground state, (b) excited state. The basal rectangular mesh designates the $(\tilde{\rho},z)$ plane where $0 \leq \tilde{\rho} \leq 4$ and $-3 \leq z \leq 3$. The nucleus of the atom is at (0,0).

Figures 4−6 depict the perspective plots of the Fukui function calculated in three strategic points representative of three zones

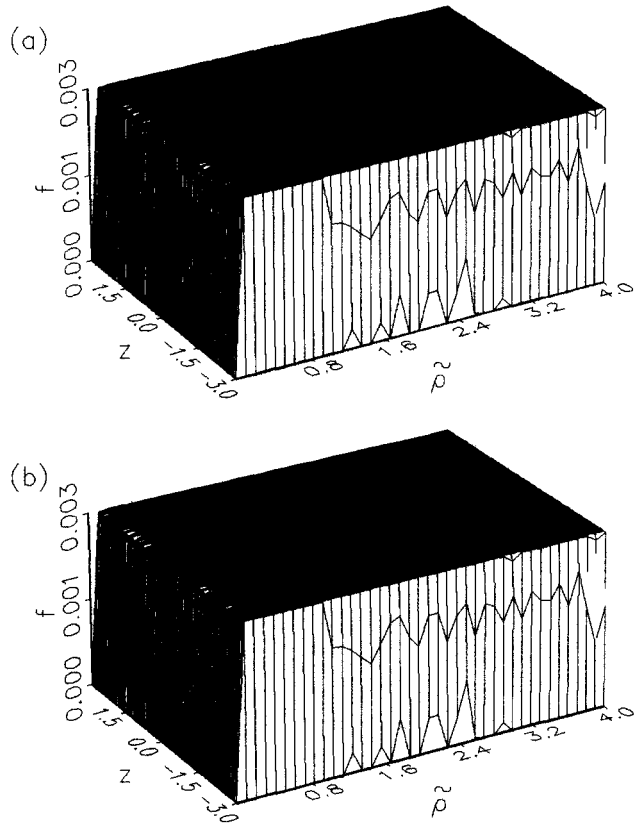

Figure 5. Perspective plots of the Fukui function of the Be atom colliding with a proton, at $t = 10.275$ au, in cylindrical polar coordinates $(\tilde{\rho},z)$: (a) ground state, (b) excited state. See caption of Figure 4 for details.

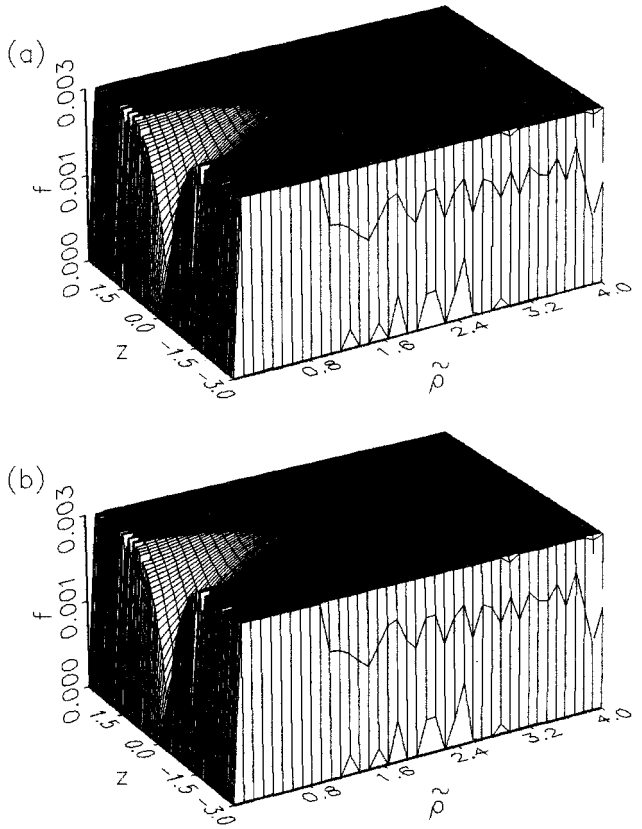

Figure 6. Perspective plots of the Fukui function of the Be atom colliding with a proton, at $t = 18.775$ au, in cylindrical polar coordinates $(\tilde{\rho},z)$: (a) ground state, (b) excited state. See caption of Figure 4 for details.

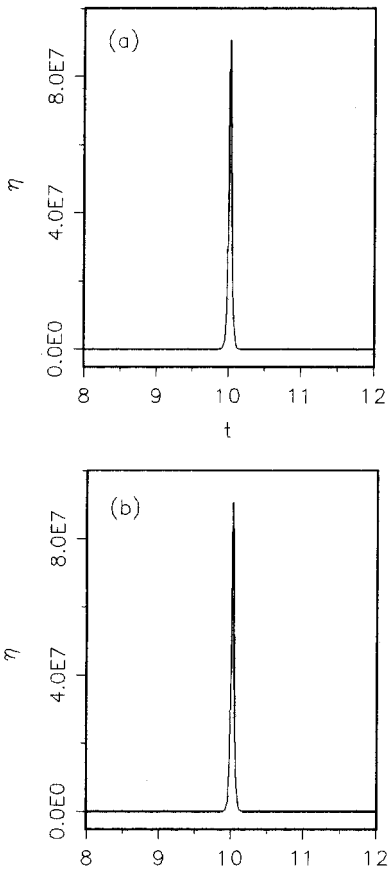

Figure 7. Time evolution of hardness (η) during a collision process between a Be atom and a proton: (a) ground state, (b) excited state

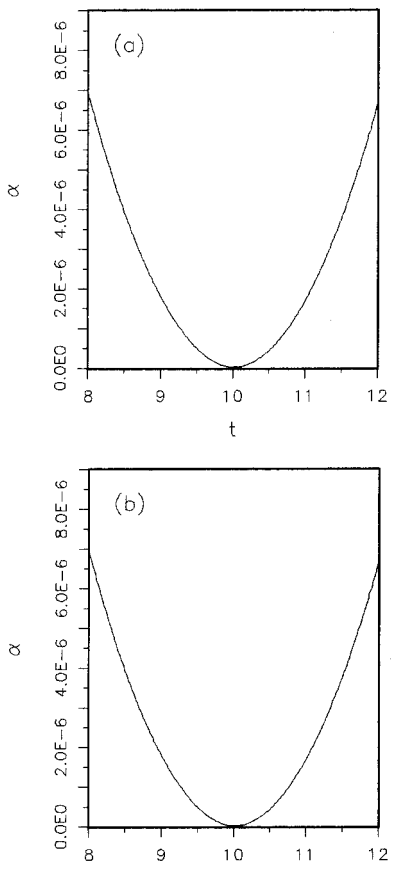

Figure 8. Time evolution of polarizability (α) during a collision process between a Be atom and a proton: (a) ground state, (b) excited state.

discussed above, viz., at the beginning of the approach regime, at the middle of the encounter regime, and toward the end of the departure regime, respectively. In Figure 4 we observe an effectively atomic $f(\tilde{\rho},z)$ when the Be atom has not started to experience the Coulomb field due to the incoming proton. When the proton proceeds toward the target, the whole scattering system starts behaving like a supermolecule and almost everywhere in space $f(\tilde{\rho},z)$ becomes significant. Once the proton and the Be atom reach their closest distance to the target, a decrease in the value of the Fukui function begins at the origin, and it becomes conspicuous when the proton moves an appreciable distance away from the target. It may be noted that $f(\tilde{\rho},z)$ is everywhere positive and normalized to unity (eq 23). The difference between these local plots for ground and excited states becomes increasingly conspicuous as time progresses. It is interesting to note that even when the proton goes to a large distance in the departure regime the Fukui function does not come back to its original shape. Presumably this occurs due to nonlinear charge oscillations since the electron density is still shared by both the nuclei. When the proton moves away it leaves behind a pulsating Be atom and the electronic charge gets continuously redistributed until it comes back completely to Be atom, leaving the free proton.

The time-dependent hardness profile is given in Figure 7. At $t = 0$, the calculated global hardness value for the ground state is 0.1898 au. Since the Be atom is yet to feel the presence of the proton it is essentially the η value for the Be atom in its ground state. This η compares very well with the corresponding literature value[49] 0.1654 au. It is important to note that this calculation of η does not require any a priori knowledge of the total or orbital energy values of the system as is the case with most of the present day prescriptions[5] for η calculations. For this reason any attempt to numerically verify the maximum hardness principle[15] (MHP) had to directly resort to the minimum energy criterion for stability. Not only are the energies not necessary for the present method but we can even bypass the solution of the Schrödinger equation in case we generate the required electron density from some other source, say from an experiment or as the solution of a single-density equation.[33,50] The initial ($t = 0$) hardness value for the excited state turns out to be 0.1875 au, which is smaller than the $\eta(t = 0)$ value for the ground state, as expected from MHP.[15] Since these two values are comparable and no unrealistic η value is obtained for the excited state, we gain some confidence in using the ground-state functionals for the excited-state calculations where almost nothing is known about the functional forms. The global hardness for both the states remain more or less static in the approach regime. In the encounter regime it suddenly increases to a very high value and passes through a maximum. It may be noted that in our earlier calculation[17] a clear-cut maximum in η profile was not observed due to the use of the homogeneous electron gas formula for $f(\mathbf{r})$. In the present calculation, *the maximization of the η profile in a dynamical situation clearly vindicates the validity of MHP[15] for both ground and excited states.* The maximum η values for these two states, respectively, are $0.906\,516\,24 \times 10^8$ and $0.906\,516\,08 \times 10^8$ au which confirms once again the MHP via the supremum η value for the ground state. After reaching the maximum value, η starts decreasing rapidly to attain a stable value in the rest of the encounter regime which is more or less the same as the static value observed in the approach regime and in the beginning of the encounter regime. The maximization of η points out that at least for a while a BeH^+ molecule is formed in the encounter regime, which eventually dissociates into Be and H^+ due to high kinetic energy of the proton. In the present context we can envisage the chemical reaction dynamics to

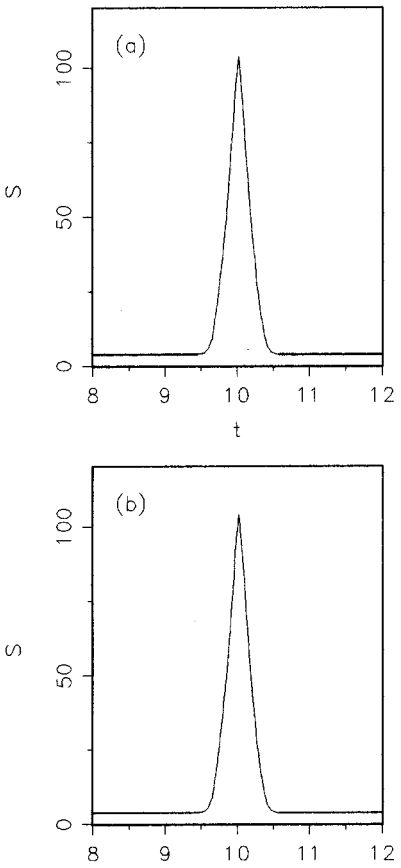

Figure 9. Time evolution of entropy (*S*) during a collision process between a Be atom and a proton: (a) ground state, (b) excited state.

follow the reaction $Be + H^+ \rightarrow BeH^+$ in time for a very low energy collision and/or a collision in the presence of another partner to take away excess collisional energy.

Figures 8 and 9 respectively depict the time dependence of polarizability and entropy associated with this collision process for both ground and excited states. At the encounter regime α becomes minimum and *S* becomes maximum which provides unmistakable signatures of the formation of BeH^+, according to the minimum polarizability principle[17] and the maximum entropy principle.[19] The minimum α values and the maximum *S* values for ground and excited states are $0.173\,082\,4 \times 10^{-7}$, $0.173\,082\,4 \times 10^{-7}$ au and 103.728 65, 103.728 64 au, respectively, as expected.

The present work demonstrates that for both ground and excited states a favorable dynamic process is characterized by maximum hardness, minimum polarizability, and maximum entropy values.

VII. Concluding Remarks

To understand the dynamical behavior of chemical reactivity indices in ground and excited states a collision process between a Be atom and a proton is studied within a quantum fluid density functional framework. A new kinetic energy functional and a new Fukui function are constructed for this purpose. The whole collision process can be divided into three distinct regimes, viz., approach, encounter, and departure in terms of the time-dependent electronegativity profile. In the encounter regime where the actual chemical process takes place, hardness maximizes, polarizability minimizes, and entropy maximizes. These results support the validity of the dynamical variants of the principles of electronegativity equalization, maximum hardness, minimum polarizability, and maximum entropy for both ground and excited states.

Acknowledgment. We would like to thank CSIR, New Delhi, for financial support. P.K.C. is grateful to Professor Robert C. Morrison and Dr. Shubin Liu for their help in various ways.

References and Notes

(1) *Electronegativity: Structure and Bonding*; Sen, K. D., Jorgenson, C. K., Eds.; Springer-Verlag: Berlin, 1987; Vol. 66.

(2) *Chemical Hardness: Structure and Bonding*; Sen, K. D., Mingos, D. M. P., Eds.; Springer-Verlag: Berlin, 1993; Vol. 80.

(3) Pauling, L. *The Nature of the Chemical Bond*, 3rd ed.; Cornell University Press: Ithaca, NY, 1960.

(4) Pearson, R. G. *Coord. Chem. Rev.* **1990**, *100*, 403; *Hard and Soft Acids and Bases*; Dowden, Hutchinson and Ross: Stroudsberg, PA, 1973.

(5) Parr, R. G.; Yang, W. *Density Functional Theory of Atoms and Molecules*; Oxford University Press: Oxford, 1989; *Annu. Rev. Phys. Chem.* **1995**, *46*, 701. Chattaraj, P. K. *J. Indian Chem. Soc.* **1992**, *69*, 173. Kohn, W.; Becke, A. D.; Parr, R. G. *J. Phys. Chem.* **1996**, *100*, 12974.

(6) Parr, R. G.; Donelly, D. A.; Levy, M.; Palke, W. E. *J. Chem. Phys.* **1978**, *68*, 3801.

(7) Parr, R. G.; Pearson, R. G. *J. Am. Chem. Soc.* **1983**, *105*, 7512.

(8) Berkowitz, M.; Ghosh, S. K.; Parr, R. G. *J. Am. Chem. Soc.* **1985**, *107*, 6811. Ghosh, S. K.; Berkowitz, M. *J. Chem. Phys.* **1985**, *83*, 2976.

(9) Parr, R. G.; Yang, W. *J. Am. Chem. Soc.* **1984**, *106*, 4049.

(10) Hohenberg, P.; Kohn, W. *Phys. Rev. B* **1964**, *136*, 864. Kohn, W.; Sham, L. J. *Phys. Rev. A* **1965**, *140*, 1133.

(11) Sanderson, R. T. *Science* **1951**, *114*, 670; *Science* **1955**, *121*, 207; *J. Chem. Educ.* **1954**, *31*, 238.

(12) Pearson, R. G. *J. Chem. Educ.* **1987**, *64*, 561; *Acc. Chem. Res.* **1993**, *26*, 250.

(13) Politzer, P.; Weinstein, H. *J. Chem. Phys.* **1979**, *70*, 3680. Parr, R. G.; Bartolotti, L. J. *J. Am. Chem. Soc.* **1982**, *104*, 3081. Nalewajski, R. F. *J. Phys. Chem.* **1985**, *89*, 2831. Mortier, W. J.; Ghosh, S. K.; Shankar, S. *J. Am. Chem. Soc.* **1986**, *108*, 4315.

(14) Chattaraj, P. K.; Lee, H.; Parr, R. G. *J. Am. Chem. Soc.* **1991**, *113*, 1855.

(15) Parr, R. G.; Chattaraj, P. K. *J. Am. Chem. Soc.* **1991**, *113*, 1854. Chattaraj, P. K.; Liu, G. H.; Parr, R. G. *Chem. Phys. Lett.* **1995**, *237*, 171. Pearson, R. G. *Chemtracts Inorg. Chem.* **1991**, *3*, 317. Liu, S.; Parr, R. G. *J. Chem. Phys.* **1997**, *106*, 5578. For a recent review, see: Chattaraj, P. K. *Proc. Indian Natl. Sci. Acad.-Part A*, **1996**, *62*, 513.

(16) Pearson, R. G. In ref 2; *Proc. Natl. Acad. Sci. U.S.A.* **1986**, *83*, 8440. Politzer, P. *J. Chem Phys.* **1987**, *86*, 1072. Ghanty, T. K.; Ghosh, S. K. *J. Phys. Chem.* **1993**, *97*, 4951. Hati, S.; Datta, D. *J. Phys. Chem.* **1994**, *98*, 10451; *J. Phys. Chem.* **1995**, *99*, 10742. Pal, S.; Chandra, A. K. *J. Phys. Chem.* **1995**, *99*, 13865.

(17) Chattaraj, P. K.; Sengupta, S. *J. Phys. Chem.* **1996**, *100*, 16126.

(18) Ghanty, T. K.; Ghosh, S. K. *J. Phys. Chem.* **1996**, *100*, 12295.

(19) Jaynes, E. T.; In *Statistical Physics*; Ford, K. W., Ed.; Brandeis Lectures, Vol. 3; Benjamin: New York, 1963. Levine, R. D.; Bernstein, R. B. In *Dynamics of Molecular Coliisions*; Miller, W. H., Ed.; Plenum Press: New York, 1976. Gadre, S. R.; Bendale, R. D. *Curr. Sci.* **1985**, *54*, 970.

(20) Chattaraj, P. K.; Nath. S. *Int. J. Quantum Chem.* **1994**, *49*, 705; *Chem. Phys. Lett.* **1994**, *217*, 342; *Proc. Indian Acad. Sci. (Chem. Sci.)* **1994**, *106*, 229. Nath, S.; Chattaraj, P. K. *Pramana* **1995**, *45*, 65.

(21) Deb, B. M.; Chattaraj, P. K. *Chem. Phys. Lett.* **1988**, *148*, 550; *Phys. Rev. A* **1989**, *39*, 1696. Chattaraj, P. K. In *Symmetries and Singularity Structures: Integrability and Chaos in Nonlinear Dynamical Systems*; Lakshmanan, M., Daniel, M., Eds.; Springer-Verlag: Berlin, 1990; pp 172−182. Deb, B. M.; Chattaraj, P. K.; Mishra, S. *Phys. Rev. A* **1991**, *43*, 1248. Chattaraj, P. K. *Int. J. Quantum Chem.* **1992**, *41*, 845. Dey, B. K.; Deb, B. M. *Int. J. Quantum Chem.* **1995**, *56*, 707.

(22) Runge, E.; Gross, E. K. U. *Phys. Rev. Lett.* **1984**, *52*, 997. Dhara, A. K.; Ghosh, S. K. *Phys. Rev. A* **1987**, *35*, 442.

(23) Madelung, E. Z. *Phys.* **1926**, *40*, 322. Deb, B. M.; Ghosh, S. K. *J. Chem. Phys.* **1982**, *77*, 342. Bartolotti, L. J. *Phys. Rev. A* **1982**, *26*, 2243.

(24) Read, S. M.; Vanderslice, J. T. *J. Chem. Phys.* **1962**, *37*, 205. Banyard, K. E.; Taylor, G. K. *J. Phys. B* **1975**, *8*, L137. Huber, K. P.; Herzberg, G. *Molecular Spectra and Molecular Structure; Constants of Diatomic Molecules*; Van Nostrand: New York, 1979; Vol. IV, p 81.

(25) Becke, A. D. *J. Chem. Phys.* **1986**, *84*, 4524.

(26) Ghosh, S. K.; Deb, B. M. *J. Phys. B* **1994**, *27*, 381.

(27) Brual, G.; Rothstein, S. M. *J. Chem. Phys.* **1978**, *69*, 1177.

(28) Kulander, K. C.; Sandhya Devi, K. R.; Koonin, S. E. *Phys. Rev. A* **1982**, *25*, 2968.

(29) Politzer, P.; Parr, R. G.; Murphy, D. R. *J. Chem. Phys.* **1983**, *79*, 3859.

(30) Chattaraj, P. K.; Deb, B. M. *J. Sci. Ind. Res.* **1984**, *43*, 238.

(31) Ludena, E. V. *J. Chem. Phys.* **1983**, *79*, 6174.

(32) Kryachko, E. S.; Ludena, E. V. *Density Functional Theory of Many-Electron Systems*; Kluwer: Dordrecht, 1990.

(33) Chattaraj, P. K. *Phys. Rev. A* **1990**, *41*, 6505.

(34) Haq, S.; Chattaraj, P. K.; Deb, B. M. *Chem. Phys. Lett.* **1984**, *111*, 79. Chattaraj, P. K.; Deb, B. M. *Chem. Phys. Lett.* **1985**, *121*, 143.
(35) Clementi, E.; Roetti, C. *At. Data Nucl. Data Tables* **1974**, *14*, 177.
(36) Murphy, D. R.; Wang, W. P. *J. Chem. Phys.* **1980**, *72*, 429.
(37) Ghosh, S. K.; Balbas, L. C. *J. Chem. Phys.* **1985**, *83*, 5778. In this paper a similar *N*-dependent correction term was introduced.
(38) Fukui, K. *Science* **1982**, *218*, 747.
(39) Chattaraj, P. K.; Cedillo, A; Parr, R. G. *J. Chem. Phys.* **1995**, *103*, 7465; *J. Chem. Phys.* **1995**, *103*, 10621 and references therein.
(40) Fuentealba, P. *J. Chem. Phys.* **1995**, *103*, 6571.
(41) Parr, R. G. *J. Phys. Chem.* **1988**, *92*, 3060.
(42) Bader, R. F. W.; McDougall, P. J.; Lau, C. D. H. *J. Am. Chem. Soc.* **1984**, *106*, 1594.
(43) *Chemical Reactivity and Reaction Path*; Klopman, G., Ed.; Wiley: New York, 1974, Chapter 4.
(44) Lee, C.; Yang, W.; Parr, R. G. *J. Mol. Struct. (THEOCHEM)* **1988**, *163*, 305.
(45) Professor Robert C. Morrison of East Carolina University has kindly supplied the ground-state and excited-state densities. He has calculated the densities from CI wave functions generated by combining Slater type orbitals of Chakravorty et al.[46] and those of Clementi and Roetti.[35] Orbitals for the dominant configuration are obtained through a self-consistent field calculation using the ATOMSCF program.[47] A multireference CI calculation with single and double excitations is then performed using the ATOMCI program.[48] The CI densities are scaled to satisfy the virial theorem followed by spherical averaging and spin tracing.
(46) Chakravorty, S. J.; Gwaltney, S. R.; Davidson, E. R.; Parpia, F. A.; Fisher, C. F. *Phys. Rev. A* **1993**, *47*, 3649.
(47) *Modern Techniques in Computational Chemistry*; Clementi, E., Ed.; ESCOM: Leiden, 1990.
(48) Saski, F.; Sekiya, M.; Noro, T; Ontsuki, K.; Osanai, Y. In *Modern Techniques in Computational Chemistry*; Clementi, E., Ed.; ESCOM: Leiden, 1990, p 181.
(49) Pearson, R. G.; *Inorg. Chem.* **1988**, *27*, 734.
(50) Chattaraj, P. K. *Chem. Phys. Lett.* **1989**, *154*, 541. Deb, B. M.; Chattaraj, P. K. *Phys. Rev. A* **1988**, *37*, 4030; *Phys. Rev. A* **1992**, *45*, 1412. For a review, see: Deb, B. M. *Proc. Indian. Natl. Sci. Acad.-Part A* **1988**, *54*, 844.